Effect of inulin on structural, physicochemical, and *in vitro* gastrointestinal tract release properties of core-shell hydrogel beads as a delivery system for vitamin B12

Min Ho Lee[a], Areum Han[a], Yoon Hyuk Chang[a]*

[a]Department of Food and Nutrition, and Bionanocomposite Research Center, Kyung Hee University, Seoul 02447, Republic of Korea

*Corresponding author. Phone: +82-2-961-0552; Fax: +82-2-961-0261;

E-mail: yhchang@khu.ac.kr

[Declarations of interest: none]

Abstract

In this study, core-shell hydrogel beads were developed as a controlled-release delivery system for vitamin B12. Vitamin B12-loaded microgels (MG) were prepared using gellan gum (GG). Core-shell hydrogel beads were produced by incorporating MG into pea protein isolate (PPI) and sodium alginate (AL) matrix filled/coated with different concentrations (0%, 1%, 3%, 5%, and 10%) of inulin (IN). Based on XRD analysis, MG was successfully incorporated into core-shell hydrogel beads. In FE-SEM and FT-IR analyses, the smoother surface and denser structure of the beads were observed as IN concentration increased due to hydrogen bonds between IN and the beads. The encapsulation efficiency increased from 68.64% to 82.36% as IN concentration increased from 0% to 10%, respectively. After exposure to simulated oral and gastric conditions, core-shell hydrogel beads exhibited a lower cumulative release than MG, and a more sustained release was observed as IN concentration increased in simulated intestinal conditions.

Keywords

Core-shell hydrogel beads, microgels, vitamin B12, *in vitro* gastrointestinal tract release properties

1. Introduction

Vitamin B12, called cyanocobalamin, is a hydrophilic micronutrient essential for red blood cell production, DNA synthesis and regulation, and cell division (Smith, Warren, & Refsum, 2018; O'Leary & Samman, 2010). Vitamin B12 deficiency is a common problem globally, which can cause anemia, neurologic disease, paralysis, and Alzheimer's disease (Stabler, 2013; Lopes, Gadelha, Carvalho, Fernandes, & Montenegro Junior, 2019). Especially, vegans and vegetarians are susceptible to vitamin B12 deficiency because the food sources of vitamin B12 are mainly confined to foods of animal origin (Rizzo & Laganà, 2020). Vitamin B12 deficiency can be prevented by oral delivery. However, even though large enough doses were given in the 100-100,000 μg range, only 1% of the vitamin B12 could be absorbed (Shipton & Thachil, 2015; Girard, Santschi, Stabler, & Allen, 2009; Kozyraki & Cases, 2013). Because vitamin B12 is structurally very sensitive to hydrochloric acid and is easily destroyed in gastric conditions before it has a chance to be absorbed in the small intestine (Morkbak, Poulsen, & Nexo, 2007; Wang et al., 2019), thus, it was indicated in this study that a controlled-release delivery system for vitamin B12 is required to improve the bioavailability of vitamin B12. Although there have been studies that encapsulate vitamin B12 to enhance its stability against environmental stress, the literature on the production of intestinal-targeted delivery systems for vitamin B12 is very few.

There have been many studies on the development of the delivery system for hydrophobic compounds; however, a few studies have been conducted on the development of the delivery system for hydrophilic compounds, such as vitamin B12 (McClements, 2015; Kurozawa & Hubinger, 2017). During the preparation of the hydrophilic compounds delivery system (hydrogels, microspheres, microgels, and so on), they tend to leak out into the external aqueous solution, subsequently leading to the lower encapsulation efficiency and the undesired initial burst release of hydrophilic compounds (Li, Li, & Zhao, 2020; Tan et al., 2019; Córdoba, Deladino, & Martino, 2013). In other words, the current challenge of the encapsulation and delivery system for hydrophilic compounds can be associated with protecting the leakage of hydrophilic compounds and inhibiting the burst release of hydrophilic compounds from the encapsulation system (Kurozawa & Hubinger, 2017). To solve this problem, this

study explored a complex and efficient matrix system that encapsulates hydrophilic compounds (vitamin B12).

Core-shell hydrogels, also known as microgel-based hydrogels, plum pudding gels, or microgel-reinforced hydrogels, are a multi-network system that entraps micro-sized hydrogels (core) inside the bulk hydrogels (shell) (Farjami & Madadlou, 2017; Bayat & Nasri, 2019). This system has several advantages for the delivery system: (1) it prevents quick elution of encapsulated compounds from the matrix, (2) it achieves targeted or sustained release profiles, and 3) it protects encapsulated compounds against environmental stress (Bayat & Nasri, 2019; Paliwal & Palakurthi, 2014). For these reasons, several studies have investigated the physicochemical and *in vitro* release properties of core-shell hydrogel matrix as an encapsulation and delivery system for hydrophilic compounds (Bayat & Nasri, 2019). Therefore, the development of core-shell hydrogel beads can be one of the effective ways to efficiently encapsulate vitamin B12 and impede the destruction of vitamin B12 in environmental stresses.

Pea protein isolate (PPI) is a non-allergenic protein that has a well-balanced essential amino acids profile and can be crosslinked with cationic ions to make a fine-stranded or particulate gel structure (Lu et al., 2020; Mession et al., 2013). Sodium alginate (SA) is a linear biopolymer of guluronic and mannuronic acids. It can be crosslinked with cationic ions such as Ca^{2+} to form egg-box-like structures (Wang et al., 2022). Besides, SA has been extensively investigated due to its biodegradability, low toxicity, and biocompatibility (Xu & Dumont, 2015). Nevertheless, PPI and SA hydrogel are permeable and susceptible to harsh chemical conditions, resulting in the burst release of encapsulated bioactive compounds in gastric conditions (Bušić et al., 2018; De Berardinis, Plazzotta, & Manzocco, 2023). However, the protein/polysaccharide-based hydrogels allow the formation of a dense matrix due to electrostatic interactions and hydrogen bonds between protein and polysaccharide, leading to the enhanced encapsulation efficiency and release profiles of encapsulated compounds (Fan, Cheng, Zhang, Zhang, & Han, 2022; Cortez-Trejo, Loarca-Piña, Figueroa-Cárdenas, Manríquez, & Mendoza, 2022). Additionally, some studies have developed delivery systems for hydrophilic compounds by

protein/polysaccharide-based hydrogels, microgels, and emulsions (Nascimento et al., 2020; Gómez-Mascaraque, Soler, & Lopez-Rubio, 2020; Kaur, Jindal, & Jindal, 2020; Comunian et al., 2013).

To enhance the encapsulation efficiency of bioactive compounds in hydrogels, some researchers have investigated the effects of filling/coating materials on the structural and physicochemical properties of hydrogel matrix systems (Moon & Chang, 2022; Córdoba, Deladino, & Martino, 2013; Li et al., 2021). In general, it was demonstrated that the addition of filling/coating material into the hydrogel matrix can reduce pores on the surface and densify the internal structure of the hydrogel matrix, consequently enhancing the encapsulation efficiency and prolonging the release profiles (Lee, Kang, & Chang, 2023; Afinjuomo et al., 2019). Some researchers noted that inulin (IN), a biocompatible natural fructan, can enhance the encapsulation efficiency and release profiles of hydrophilic compounds when it was added to the hydrogel matrix as filling/coating materials (Stojanovic et al., 2012; Balanč et al., 2016). For these reasons, IN was used as a filling/coating material in the present study to reinforce core-shell hydrogel beads.

In the present study, a novel carrier (core-shell hydrogel beads) for the delivery system for vitamin B 12 was prepared, and it consists of gellan gum (GG) microgels as core materials and PPI/SA hydrogels filled/coated with IN as shell materials. An additional physical barrier to GG microgels was expected to enhance the encapsulation efficiency and prevent the undesired release of vitamin B12. Furthermore, it was hypothesized that adding IN to the core-shell hydrogel matrix would improve the encapsulation efficiency and release profiles of vitamin B12 by reinforcing the hydrogel structure. Accordingly, the objectives of this study were (1) to prepare vitamin B12-loaded microgels using GG, (2) to develop core-shell hydrogel beads filled/coated with different concentrations of IN as a controlled-release delivery system for vitamin B12, and (3) to evaluate the structural, physicochemical, and *in vitro* gastrointestinal release properties of the core-shell hydrogel beads.

2. Materials and methods

2.1. Materials

Gellan gum (GG) and sodium alginate (SA) were purchased from ES Food (Gunpo, Korea). Pea protein isolate (PPI) was purchased from Emsland-Starke GmbH (Emlichheim, Germany). Inulin (IN) was obtained from NOW Foods (Bloomingdale, IL, USA). Vitamin B12, pepsin from porcine (P7012, powder, ≥2500 units/mg solid), bile salt (B8765), and pancreatin from porcine pancreas (P7545, 8×USP specifications) were purchased from Sigma Aldrich Chemical Co. (St. Louis, MO, USA). All other chemicals used were of analytical grade.

2.2. Preparation of vitamin B12-loaded microgels (MG)

Microgels (MG) were prepared by the method of Ellis & Jacquier (2009) with some modifications. To prepare GG and vitamin B12 mixture, GG (3%, w/w) and vitamin B12 (0.1%, w/w) were dissolved in distilled water at 80 °C under magnetic stirring for 30 min. Then, 100 g of preheated soybean oil (80 °C) was poured into 30 g of GG and vitamin B12 mixture and stirred at 80 °C for 1 h (500 rpm). Following the preparation of the emulsified GG and vitamin B12 mixture, the emulsified mixture was cooled at 5 °C under magnetic stirring for 1 h (300 rpm). During the process, GG formed a gel particle. Subsequently, the final mixture was centrifugated at 500×g for 5 min to remove soybean oil. The precipitate was washed with 200 mL of Tween 80 (1%, w/w) and 200 mL of distilled water. Finally, the precipitate was filtered with Whatman No.1 paper to obtain MG. The MG was stored at 4 °C for further analysis.

2.3. Preparation of core-shell hydrogel beads filled/coated with inulin (IN)

Core-shell hydrogel beads were prepared according to the method of Ozel, Zhang, He, & McClements (2020) with some modifications. Firstly, PPI solution (15%, w/w) and AL solution (2%, w/w) were prepared by dissolving PPI and AL in distilled water at 80 °C, respectively. After completely dissolving, each solution was cooled at 5 °C for 30 min. Then, the pH of PPI solution was adjusted to 7.0 with glacial acetic acid and mixed with AL solution in a 1:1 ratio (w/w). The different concentrations (0%, 1%, 3%, 5%, and 10%, w/w) of IN were dissolved in the PPI and AL mixture. MG (10%, w/w) was added to the PPI and AL mixture with different concentrations of IN. Subsequently, the mixture

was added dropwise into $CaCl_2$ solution (5%, w/w) by using a syringe without a needle and stirring for 10 min at 300 rpm to obtain core-shell hydrogel beads. Core-shell hydrogel beads were washed with distilled water and filtered with Whatman No.1. The core-shell hydrogel beads were stored at 4 °C for further analysis. Based on the different concentrations (0%, 1%, 3%, 5%, and 10%) of IN, core-shell hydrogel beads were referred to as MG/PPI/AL/IN_0-HG beads, MG/PPI/AL/IN_1-HG beads, MG/PPI/AL/IN_3-HG beads, MG/PPI/AL/IN_5-HG beads, and MG/PPI/AL/IN_{10}-HG beads.

2.4. Field emission scanning electron microscopy (FE-SEM) analysis

The surface morphologies and microstructure of MG and core-shell hydrogel beads were observed by Field Emission Scanning Electron Microscope (FE-SEM, S-4700, Hitachi High-Technologies, Tokyo, Japan). The samples were coated and observed at an acceleration voltage of 10 kV with a magnification of 30–200. Before observation, all samples were lyophilized using a freeze dryer (FD8508, Ilshin Biobase Co. Ltd., Gyeonggi, Korea) and passed through a 180 μm mesh standard sieve.

2.5. X-ray diffraction (XRD) analysis

XRD patterns of MG and core-shell hydrogel beads were recorded by X-ray diffractometer (X'Pert PRO, Malvern Panalytical Ltd., Malvern, UK) with a Cu Kα radiation (λ=1.54060 Å). All samples were scanned at a diffraction angle of 2θ from 10° to 60° at the scanning rate of 1° per minute. The X-ray generator was operated at 40 kV and 40 mA. Before observation, all samples were lyophilized and passed through a 180 μm mesh standard sieve. GG, vitamin B12, PPI, AL, and IN were determined as controls.

2.6. Fourier transform infrared (FT-IR) spectroscopy analysis

FT-IR spectra of MG and core-shell hydrogel beads were analyzed by FT-IR spectrophotometer (ATR

PRO 4X FTIR spectrophotometer, Jasco, Japan) with an ATR sampling accessory. All spectra in the 4,000-500 cm^{-1} range were scanned at 4 cm^{-1} resolution. Before observation, all samples were

lyophilized and passed through a 180 μm mesh standard sieve. GG, vitamin B12, PPI, AL, and IN were determined as controls.

2.7. Quantification of vitamin B12

Quantification of vitamin B12 concentration between 1 mg/mL and 100 mg/mL was determined by the method of Sarti et al. (2013) with some modifications using high-performance liquid chromatography (HPLC, Agilent 1100 series, Agilent Technologies, Palo Alto, CA, USA) with a diode array detector at 360 nm. Agilent Eclipse XDB-C18 column (4.6 X 150mm, packed with 5 μm particles) was used for chromatographic separation at a flow rate of 0.7 mL/min. The mobile phase consisted of solvents A: formic acid in water (0.1%, v/v) and B: formic acid in acetonitrile (0.1%, v/v). Solvents A and B were run for 3 min in a 90:10 ratio. Subsequently, a gradient phase from 90:10 to 50:50 ratio was eluted for 27 min. In the following 5 min, solvents A and B were brought to the 90:10 ratio and held constant for 10 min. The injection volume was 10μL. The amount of vitamin B12 in the sample was calculated from the standard curve (1-100 mg/mL of free vitamin B12).

2.8. Encapsulation efficiency of vitamin B12

The encapsulation efficiency of MG and core-shell hydrogel beads was determined according to the method of Mazzocato, Thomazini, & Favaro-Trindade (2019) with some modifications. 1 g of MG and core-shell hydrogel beads were dispersed in 9 g of distilled water, followed by homogenization at 17,500 rpm for 1 min. The suspension was centrifuged at 3,500 rpm for 10 min. The supernatant was filtered with a 0.22 μm pore size nylon filter and injected into HPLC for vitamin B12 quantification (section 1.2.5). All samples were measured in triplicate. The encapsulation efficiency was calculated by the following equation:

Encapsulation efficiency (%) = $(W_0 / W_t) \times 10$

Where W_t is the amount of added vitamin B12 in samples, and W_0 is the amount of encapsulated vitamin B12 in samples.

2.9. Zeta potential analysis

The zeta potential of PPI solution (15%, w/w) and AL solution (2%, w/w) was measured according to the method of Luo et al. (2022) with some modifications. The prepared PPI and AL solution were adjusted to pH values of 3.0 and 7.0 using 1 N HCl or 1 N NaOH. The zeta potential of samples was measured by Zetasizer Nano ZSP (Malvern Instruments, Worcestershire, UK) under different pH conditions. All tests were performed at 25°C and determined in triplicates.

2.10. Swelling ratio analysis

The swelling ratio of MG and core-shell hydrogel beads was measured based on the method of Yang, Liang, Xiang, & Situ (2021) with some modifications. 0.5 g of MG and core-shell hydrogel beads were soaked in 20 mL of PBS buffer (pH 3.0 and 7.0) in a 37 °C water bath. After 2 h, the swollen sample was filtered with Whatman No.3 and weighed. All samples were measured in triplicate. The swelling ratio of MG and core-shell hydrogel beads was calculated by the following equation:

$$\text{Swelling ratio (\%)} = (W_t - W_0) / W_0 \times 100$$

Where W_t is the weight of the swollen samples, and W_0 is the weight of the samples before swelling.

2.11. *In vitro* release study of encapsulated vitamin B12 in simulated gastrointestinal conditions

The *in vitro* gastrointestinal release properties of MG and core-shell hydrogel beads in simulated oral, gastric, and intestinal conditions were sequentially performed according to the INFOGEST static *in vitro* model (Brodkorb et al., 2019). Simulated salivary fluid (SSF), simulated gastric fluid (SGF), and simulated intestinal fluid (SIF) were prepared based on the method of Minekus et al. (2014). All reagents were preheated at 37 °C before use. The digestion fluids were collected and replaced with an equal volume of fresh media after each digestion step. Collected fluids were centrifugated at 3,500 rpm for 10 min. The supernatant was filtered with a 0.22 μm pore size nylon filter and injected into HPLC for vitamin B12 quantification (section 1.2.6). All samples were measured in triplicate. The release rate of vitamin B12 was calculated by the following equation:

$$\text{Release rate (\%)} = (W_0 / W_t) \times 100$$

Where W_t is the amount of encapsulated vitamin B12 in samples, and W_0 is the amount of released vitamin B12 after the digestion step

2.11.1. Simulated oral conditions

To simulate oral conditions, MG and core-shell hydrogel beads (0.5 g) were dispersed in 2.0 mL of ultrapure water, followed by mixed with 2 mL of SSF, 487.5 μL of ultrapure water, and 12.5 uL of 0.3 M $CaCl_2$ solution. The mixture was adjusted to pH 7.0 using 1 N HCl and agitated at 100 rpm for 2 min at 37 °C.

2.11.2 Simulated gastric conditions

A total of 5 mL of oral bolus were mixed with 3.75 mL of SGF, 0.8 mL of pepsin solution (2,000 U/mL in the gastric mixture), 100 μL of 1 N HCl, 2.5 μL of 0.3 M $CaCl_2$, and 347.5 μL of ultrapure water. The mixture was adjusted to pH 3.0 using 1 N HCl and agitated at 100 rpm for 120 min at 37 °C.

2.11.3. Simulated intestinal conditions

A total of 10 mL of gastric chyme were mixed with 5.5 mL of SIF, 2.5 mL of pancreatin solution (100 U/mL in the intestinal mixture), 1.25 mL of 160 mM bile salt solution, 75 μL of 1 N NaOH, 0.655 mL of ultrapure water, and 20 uL of 0.3 M $CaCl_2$ solution. The mixture was adjusted to pH 7.0 using 1 N NaOH and agitated at 100 rpm for 120 min at 37 °C.

2.12. Storage stability

The storage stability of vitamin B12 in MG and core-shell hydrogel beads was evaluated according to the method of Dutta & Bhattacharjee (2017) with slight modifications. MG and core-shell hydrogel beads were added to each tube and stored at 4 °C for 14 days. The amount of vitamin B12 retained in MG and core-shell hydrogel beads was determined on days 7 and 14 using the methods described in Section 1.2.6. All samples were measured in triplicate. The storage stability of vitamin B12 was calculated by the following equation:

Release rate (%) = (W_0 / W_t) × 100

Where W_t is the amount of vitamin B12 before storage, and W_0 is the amount of vitamin B12 remained at different storage times.

2.13. Statistical analysis

All statistical analyses were performed using SPSS 26.0 (SPSS Inc., Chicago, IL, USA). Analysis of variance (ANOVA) was performed using the general linear models (GLM) procedure to determine significant differences among the samples. Means were compared by using Fisher's least significant difference (LSD) procedure. Significance was defined at the 5% level (p<0.05).

3. Results and discussion

3.1. Field emission scanning electron microscopy (FE-SEM) analysis

Fig. 1 shows the FE-SEM images of MG and core-shell hydrogel beads filled/coated with different concentrations of IN. In the case of MG, non-spherical shapes with wrinkles on the surface were observed.

In surface images, core-shell hydrogel beads showed a rough surface with some pores. It can be attributed to lyophilization, which can cause structural changes in core-shell hydrogel beads to become shrunken and porous (Yao et al., 2017). However, as IN concentration was increased, fewer pores were observed in core-shell hydrogel beads. Liu et al. (2022) also reported that the increasing concentrations of IN decreased the surface pores of AL hydrogel beads because IN coated the hydrogel beads.

Cross-sectional images showed that the internal structure of core-shell hydrogel beads became denser with the increase in IN concentrations. Wang, Luo, & Xiao (2021) reported that as concentrations of starch filler increased, the internal structure of oxidized GG-based hydrogel became gradually denser. In addition, Chan et al. (2011) reported that when starch was added to AL hydrogel beads, the internal structure of the AL hydrogel beads became denser because the starch filler occupied the internal structure of AL hydrogel beads. Accordingly, it was indicated in the present study that adding IN as filling/coating materials was able to coat and fill the surface and internal structure of core-shell hydrogel

beads, and the increase in the concentrations of IN made the core-shell hydrogel beads denser and fewer pores.

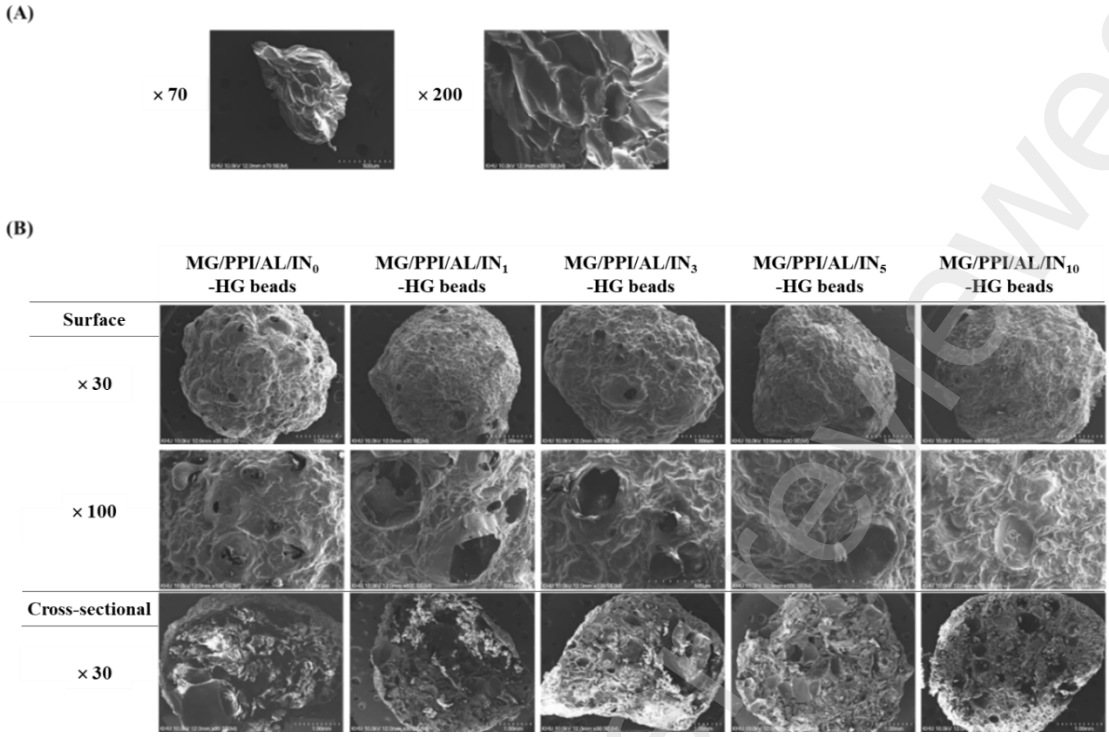

Fig. 1. Field emission scanning electron microscope (FE-SEM) images of (A) microgels (MG) and (B) core-shell hydrogel beads prepared with different concentrations of inulin (IN). MG/PPI/AL/IN_0-HG beads, MG/PPI/AL/IN_1-HG beads, MG/PPI/AL/IN_3-HG beads, MG/PPI/AL/IN_5-HG beads, and MG/PPI/AL/IN_{10}-HG beads represent core-shell hydrogel beads prepared with different concentrations of IN (0%, 1%, 3%, 5%, and 10%, respectively).

3.2. X-ray diffraction (XRD) analysis

The XRD patterns of vitamin B12, GG, MG, PPI, AL, IN, and core-shell hydrogel beads filled/coated with different concentrations of IN are shown in Fig. 2. Vitamin B12 had an amorphous structure with no peaks, which was in line with previous report by Khodaverdi et al. (2014). GG had a characteristic peak at around 19°, indicating the semi-crystalline structure of GG as previously reported in the literature (Mahmood et al., 2021). MG showed a similar XRD pattern to GG. Fang et al. (2023) reported that the thermo-reversible gelation of carrageenan did not affect the crystalline structure of carrageenan because no significant changes were observed in the XRD peaks of carrageenan after the gelation process. Thus, it was assumed in this study that MG exhibited a similar XRD pattern to GG because the crystalline structure of GG did not change after the gelation process.

The characteristic peak of MG disappeared in all core-shell hydrogel beads, indicating that MG was successfully incorporated into the hydrogel matrix. Chen et al. (2020) also noted that the absence of the characteristic XRD patterns for zein microgels in core-shell hydrogel beads could be related to the successful incorporation of microgels into the hydrogel matrix.

PPI and AL had characteristic peaks at 19° (Guo et al., 2020) and 13° (Rathna, Birajdar, Bhagwani, & Paul, 2013), respectively. However, the characteristic peaks of PPI and AL were not observed in all core-shell hydrogel beads, indicating that PPI and AL were transformed from a crystalline structure to an amorphous structure. This phenomenon may be related to the rearrangement of molecular conformations induced by hydrogen bonds and electrostatic interactions between PPI and AL (Zhou et al., 2020; Wu et al., 2023). Wu et al. (2023) reported that the molecular interactions between AL and whey protein can rearrange the molecular conformation, forming an amorphous hydrogel structure. Therefore, it was suggested in this study that PPI and AL were transformed to an amorphous structure due to intermolecular interactions; consequently, core-shell hydrogel beads showed an amorphous structure.

IN showed a broad peak around 18°, indicating the amorphous structure of IN (Saavedra-Leos et al., 2014; Ronkart, Paquot, Fougnies, Deroanne, & Blecker, 2009). There was no significant difference in the XRD patterns between the core-shell hydrogel beads without the addition of IN (MG/PPI/AL/IN_0-

306 HG) and the core-shell hydrogel beads filled/coated with IN (MG/PPI/AL/IN_1-HG, MG/PPI/AL/IN_3-
307 HG, MG/PPI/AL/IN_5-HG, MG/PPI/AL/IN_{10}-HG). It was suggested that IN did not affect the amorphous
308 structure of core-shell hydrogel beads. This behavior agrees with the observation of Ji et al. (2021), who
309 evaluated the influence of IN on the XRD patterns of pea starch gels.
310

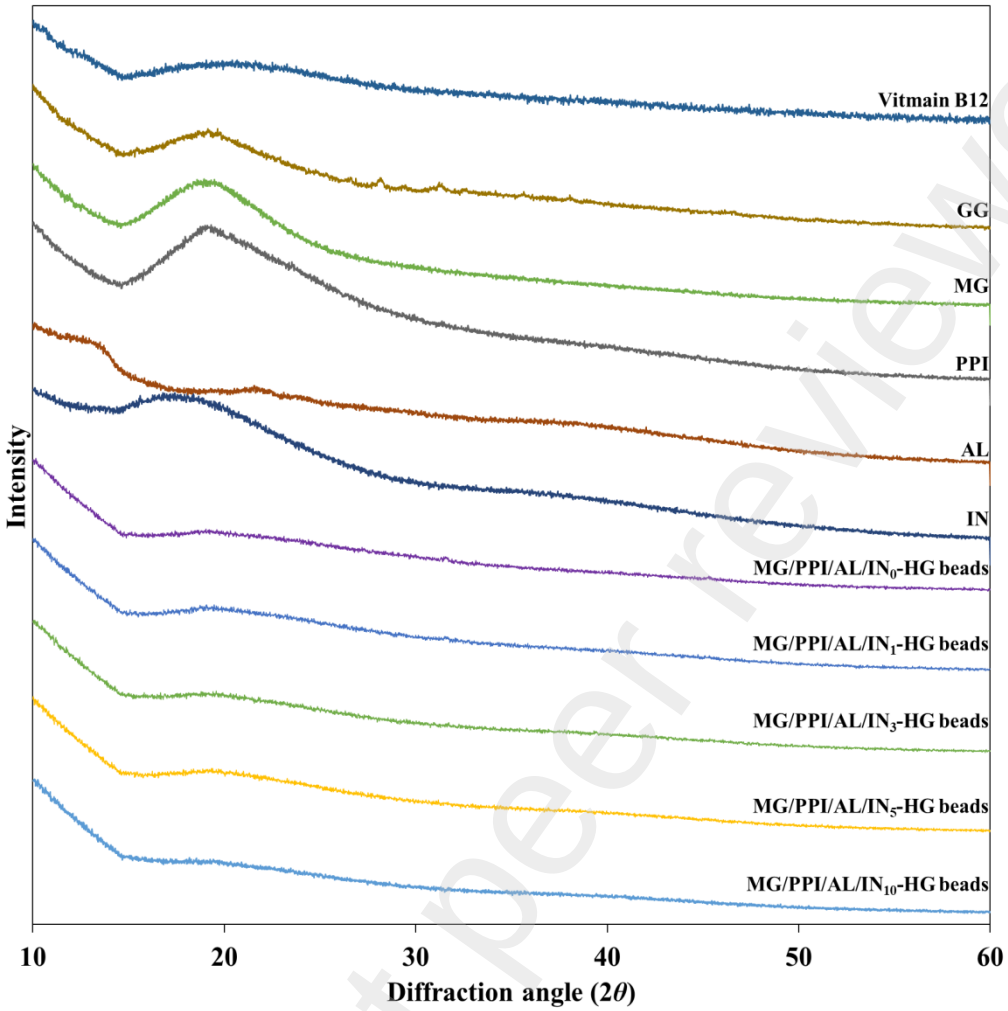

311

312 **Fig. 2.** X-ray diffraction (XRD) patterns of vitamin B12, gellan gum (GG), microgels (MG), pea protein
313 isolate (PPI), sodium alginate (AL), inulin (IN), and core-shell hydrogel beads prepared with different
314 concentrations of IN. MG/PPI/AL/IN_0-HG beads, MG/PPI/AL/IN_1-HG beads, MG/PPI/AL/IN_3-HG
315 beads, MG/PPI/AL/IN_5-HG beads, and MG/PPI/AL/IN_{10}-HG beads represent core-shell hydrogel beads
316 prepared with different concentrations of IN (0%, 1%, 3%, 5%, and 10%, respectively).

317

3.3. Fourier transform infrared (FT-IR) spectroscopy analysis

The FT-IR spectra of vitamin B12, GG, MG, PPI, AL, IN, and core-shell hydrogel beads are represented in Fig. 3. Fig. 3A shows the FT-IR spectra of vitamin B12, GG, and MG. The characteristic peaks of vitamin B12 were found at 1573 cm^{-1} and 1657 cm^{-1}, which corresponded to the amide I (C=O stretching vibration) of the propionamide side chains of the corrin ring, and C–C stretching vibration of the corrin ring, respectively (Jin, Lu, You, Chen, & Dong, 2009; Estevinho, Carlan, Blaga, & Rocha, 2016). The characteristic peaks of vitamin B12 were not observed in MG, suggesting that vitamin B12 was successfully encapsulated into MG.

In the case of GG, characteristic peaks were found at 3125 cm^{-1}, 1596 cm^{-1}, and 1405 cm^{-1}. The peak at 3125 cm^{-1} corresponded to O–H stretching vibration (Karthika, Vishalakshi, & Naik, 2016). The peaks at 1596 cm^{-1} and 1405 cm^{-1} were attributed to the $–COO^-$ asymmetric and $–COO^-$ symmetric stretching vibrations of carboxylate ion, respectively (Bonifacio, Gentile, Ferreira, Cometa, & De Giglio, 2017; Mundlia, Ahuja, & Kumar, 2021). The peak at 1030 cm^{-1} was assigned to the C–O stretching vibration (Bonifacio, Gentile, Ferreira, Cometa, & De Giglio, 2017).

In the FT-IR spectrum of MG, major characteristic peaks were observed at 3281 cm^{-1}, 1602 cm^{-1}, and 1455 cm^{-1}. The absorption band at 3281 cm^{-1} indicated O–H stretching vibration peak. The peaks at 1602 cm^{-1} and 1455 cm^{-1} were attributed to $–COO^-$ asymmetric stretching vibration and $–COO^-$ symmetric stretching vibration, respectively. The characteristic peaks at 3125 cm^{-1}, 1596 cm^{-1}, and 142 cm^{-1} of GG were shifted to the higher wavenumber in MG, which may be related to the intermolecular crosslinking of GG chains. de Souza et al. (2016) prepared GG thermo-reversible hydrogels and reported that the peaks of O–H, $–COO^-$ asymmetric, and $–COO^-$ symmetric stretching vibration of GG were shifted to a higher wavenumber because the increasing intermolecular interactions in GG chains, leading to double helix structure.

The FT-IR spectra of PPI, AL, IN, and core-shell hydrogel beads are shown in Fig. 3B. PPI showed major characteristic peaks at 3268 cm^{-1}, 1670 cm^{-1}, and 1518 cm^{-1} in the FT-IR spectrum, which corresponded with O–H stretching vibrations, amide I, and amide II, respectively (Shevkani, Singh, Kaur, & Rana, 2015; Mozafarpour & Koocheki, 2023). In the FT-IR spectrum of AL, major

characteristic peaks were found at 3123 cm^{-1}, 1599 cm^{-1}, and 1518 cm^{-1}, which were attributed to O–H, $–COO^-$ asymmetric, and $–COO^-$ symmetric stretching vibration, respectively (Ionita, Pandele, & Iovu, 2013).

In the FT-IR spectrum of core-shell hydrogel beads, the amide I peak of PPI (1670 cm^{-1}) shifted to lower wavenumbers (1630 cm^{-1}-1638 cm^{-1}) and overlapped with the peak of free carboxyl groups in AL (1599 cm^{-1}). Byeon, Kang, & Chang (2023) observed that the amide I peak of gelatin overlapped with the peak of the free carboxyl groups of low methoxyl pectin, and they reported that this phenomenon was related to strong intermolecular interactions such as hydrogen bonds and electrostatic interactions between gelatin and low methoxyl pectin. Similar results were also observed by Wang et al. (2022), who developed PPI and AL hydrogel beads. They (Wang et al., 2022) reported that the amide I peak of PPI shifted to a lower wavenumber and overlapped with the peak of free carboxyl groups in AL, indicating the existence of non-covalent interactions between PPI and AL. Therefore, it was suggested in the present study that non-covalent interactions (hydrogen bonds and electrostatic interaction) can be formed between PPI and AL in core-shell hydrogel beads.

IN had major characteristic peaks at 3264 cm^{-1}, 2938 cm^{-1}, and 1418 cm^{-1} in the FT-IR spectrum, which were caused by the O–H stretching vibration, C–H stretching vibration, and internal deformations of CH_2–OH groups on the fructose ring, respectively (Apolinário et al., 2017; Panchev, Delchev, Kovacheva, & Slavov, 2011; López-Molina et al., 2015). As the concentration of IN was increased from 0% to 10%, the O–H stretching vibration peak of core-shell hydrogel beads around 3200 cm^{-1} shifted to a lower wavenumber (3264 cm^{-1}-3221 cm^{-1}), indicating the formation of hydrogen bonds between IN and core-shell hydrogel beads. However, there were no changes in the FT-IR spectrum after filling or coating IN into core-shell hydrogel beads, suggesting that covalent bonds were not formed between IN and core-shell hydrogel beads. Ji et al. (2021) developed pea starch gel with different concentrations of IN and reported that no new peaks were found with an increase in IN concentrations, and the O–H stretching vibration peak was shifted to a lower wavenumber, which meant that no covalent bonds formed and hydrogen bond was existed between IN and pea starch.

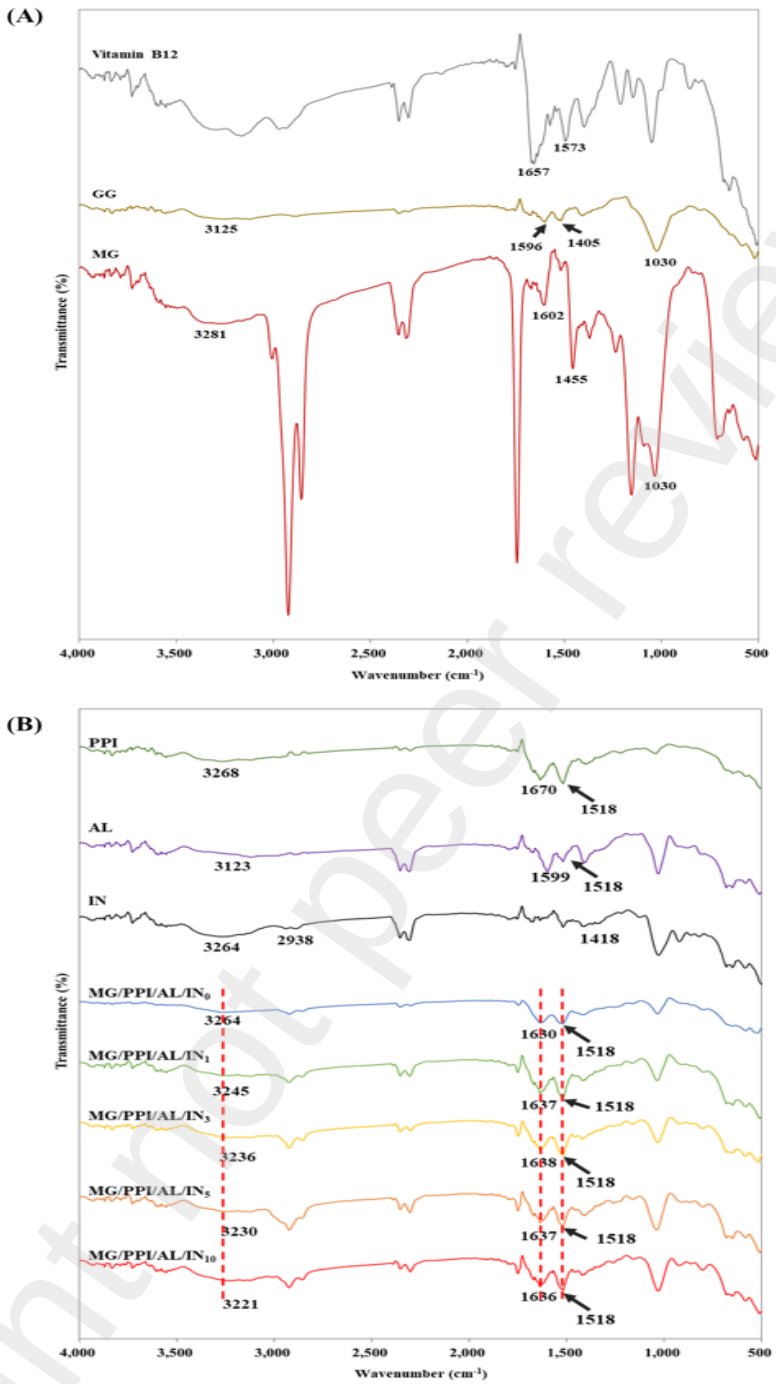

Fig. 3. FT-IR spectra of (A) vitamin B12, gellan gum (GG), and microgel (MG), and (B) pea protein isolate (PPI), sodium alginate (AL), inulin (IN), and core-shell hydrogel beads prepared with different concentrations of IN. MG/PPI/AL/IN_0-HG beads, MG/PPI/AL/IN_1-HG beads, MG/PPI/AL/IN_3-HG beads, MG/PPI/AL/IN_5-HG beads, and MG/PPI/AL/IN_{10}-HG beads represent core-shell hydrogel beads prepared with different concentrations of IN (0%, 1%, 3%, 5%, and 10%, respectively).

3.4. Encapsulation efficiency of vitamin B12

Table 1 represents the encapsulation efficiency of vitamin B12 in MG and core-shell hydrogel beads. The encapsulation efficiency of vitamin B12 in MG was 83.58%. According to FT-IR analysis, MG was produced by a conformational change of GG during thermo-reversible gelation, which can lead to a relatively high encapsulation efficiency.

The encapsulation efficiency of vitamin B12 in core-shell hydrogel beads was lower than MG. According to Mirmazloum et al. (2021), the low encapsulation efficiency of core-shell hydrogel beads is attributed to the diffusion of the encapsulated compounds into the gelling solution while manufacturing core-shell hydrogel beads. However, the encapsulation efficiency of vitamin B12 in core-shell hydrogel beads was increased from 68.64% to 82.36%, increasing the concentration of IN from 0% to 10%, respectively. It may be related to the increased concentration of IN in the core-shell hydrogel beads, which formed a denser structure and fewer pores of core-shell hydrogel beads. Cortés-Camargo et al. (2023) reported that the use of tamarind mucilage as filling materials for producing AL hydrogel beads enhanced the encapsulation efficiency of sesame oil because tamarind mucilage acted as filling materials to prevent the diffusion of sesame oil. Based on the FE-SEM and FT-IR results that were previously mentioned, IN filled the internal structure and coated the surface of core-shell hydrogel beads via hydrogen bonds. Accordingly, the addition of IN to the core-shell hydrogel beads can reinforce the structure by filling the internal matrix and coating the surface of the hydrogel beads. It ultimately can improve the encapsulation efficiency of vitamin B12.

399 **Table 1. Encapsulation efficiency of microgels (MG) and core-shell hydrogel beads prepared**

400 **with different concentrations of inulin (IN).**

Samples	Encapsulation efficiency (%)
MG	83.58 ± 0.42^{a}
MG/PPI/AL/IN_0-HG beads	68.64 ± 0.90^{e}
MG/PPI/AL/IN_1-HG beads	71.96 ± 0.24^{d}
MG/PPI/AL/IN_3-HG beads	75.37 ± 1.51^{c}
MG/PPI/AL/IN_5-HG beads	78.05 ± 1.06^{b}
MG/PPI/AL/IN_{10}-HG beads	82.36 ± 0.67^{a}

MG/PPI/AL/IN_0 -HG beads, MG/PPI/AL/IN_1 -HG beads, MG/PPI/AL/IN_3 -HG beads, MG/PPI/AL/IN_5 -HG beads, and MG/PPI/AL/IN_{10} -HG beads represent core-shell hydrogel beads prepared with different concentrations of IN (0%, 1%, 3%, 5%, and 10%, respectively).

Values with the same letters within the same columns are not significantly different ($p<0.05$).

401

3.5. Zeta potential analysis

Fig. 4 shows the zeta potential of PPI and AL at pH 3.0 and 7.0. At pH 3.0, the zeta potential of PPI was +13.5 mV, and AL exhibited a zeta potential of -21.67 mV, indicating that the protonation of amine groups in PPI and deprotonation of carboxyl groups in AL can occur. Bishnoi, Trvifol, Moriana, & Mendes (2022) also reported that the protonated amine groups of whey protein isolate and deprotonated carboxyl groups in AL occurred at pH 3.0.

At pH 7.0, PPI and AL had zeta potentials of -12.83 mV and -34.97 mV, respectively. The deprotonation of carboxyl groups in AL was more predominant at pH 7.0 than at pH 3.0 because the zeta potential of AL was lower at pH 7.0 than at pH 3.0. Additionally, deprotonation of carboxyl groups in PPI was observed at pH 7.0.

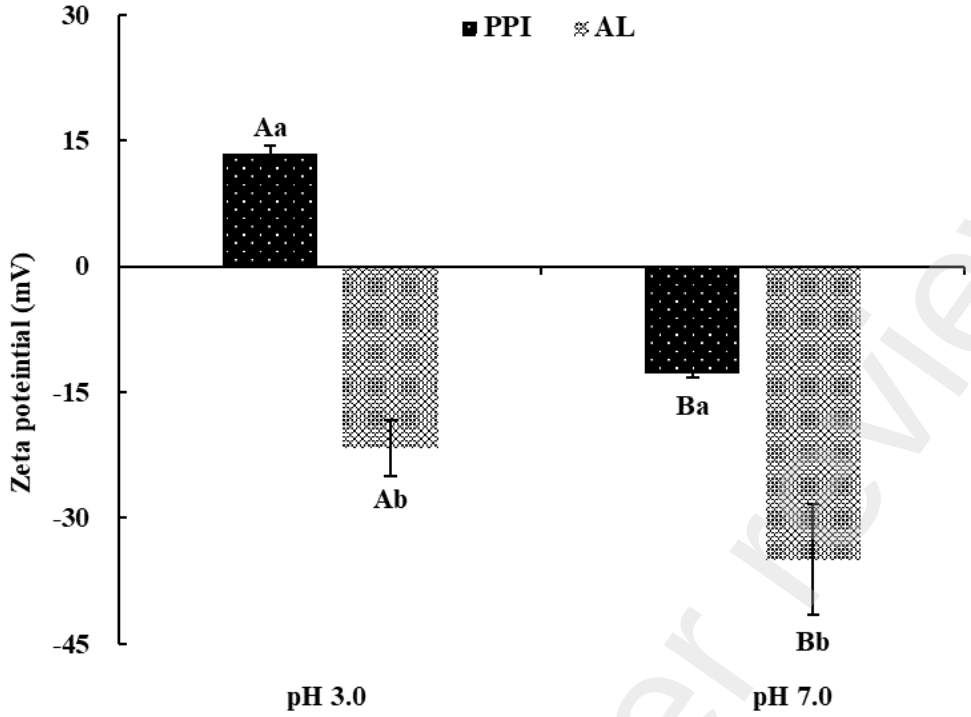

413

414 **Fig. 4.** Zeta potential of pea protein isolate (PPI) and sodium alginate (AL) solutions at pH 3.0 and 7.0.

415 Lowercase letters show significant differences among samples at the same pH (p<0.05) and capital

416 letters show significant differences among pH for the same sample (p<0.05).

417

3.6. Swelling ratio analysis

The swelling ratio of MG and core-shell hydrogel beads at pH 3.0 and pH 7.0 is represented in Fig. 5. The swelling ratio of core-shell hydrogel beads at pH 3.0 was lower than that at pH 7.0. According to the zeta potential analysis (Fig. 4), amine groups of PPI can be protonated, and carboxyl groups of AL can be deprotonated at pH 3.0. Subsequently, it was assumed that electrostatic repulsion between carboxyl groups ($–COO^-$) can be reduced, and electrostatic interactions between cationic groups of PPI (NH_3^+) and anionic groups of AL ($–COO^-$) can be preferred, causing the restricted swelling of core-shell hydrogel beads at pH 3.0. However, at pH 7.0, both PPI and AL exhibited net negative charges (carboxyl groups in both PPI and AL were deprotonated into anionic forms), and the zeta potential of AL was lower than that at pH 3.0. Therefore, electrostatic repulsion between carboxyl groups ($–COO^-$) increased, and the swelling ratio of core-shell hydrogel beads at pH 7.0 was higher than that at pH 3.0. A similar result has been found by Ozel et al. (2020). They reported that the swelling ratio of PPI/carrageenan hydrogels was decreased at pH 3.0 due to the decrease of electrostatic repulsion in anionic groups of AL and the occurrence of electrostatic interactions between cationic groups of PPI and anionic groups of carrageenan. However, at pH 7.0, the swelling ratio increased due to electrostatic repulsion between PPI and AL anionic groups.

No significant difference in the swelling ratio was observed between core-shell hydrogel beads in an acidic medium (pH 3.0). However, in a neutral medium (pH 7.0), the swelling ratio decreased from 12.84% to 7.94%, increasing IN concentration from 0% to 10%. According to Wang et al. (2021), a lower swelling ratio was found for GG hydrogel beads as the concentrations of added resistant starch increased. They suggested that adding resistant starch to hydrogel beads can weaken the electrostatic repulsion forces between carboxyl groups in GG and reduce the swelling ratio. Accordingly, in this study, the addition of IN can reduce the forces of electrostatic repulsion between anionic groups ($–COO^-$) of PPI and AL, which leads to a decreasing swelling ratio.

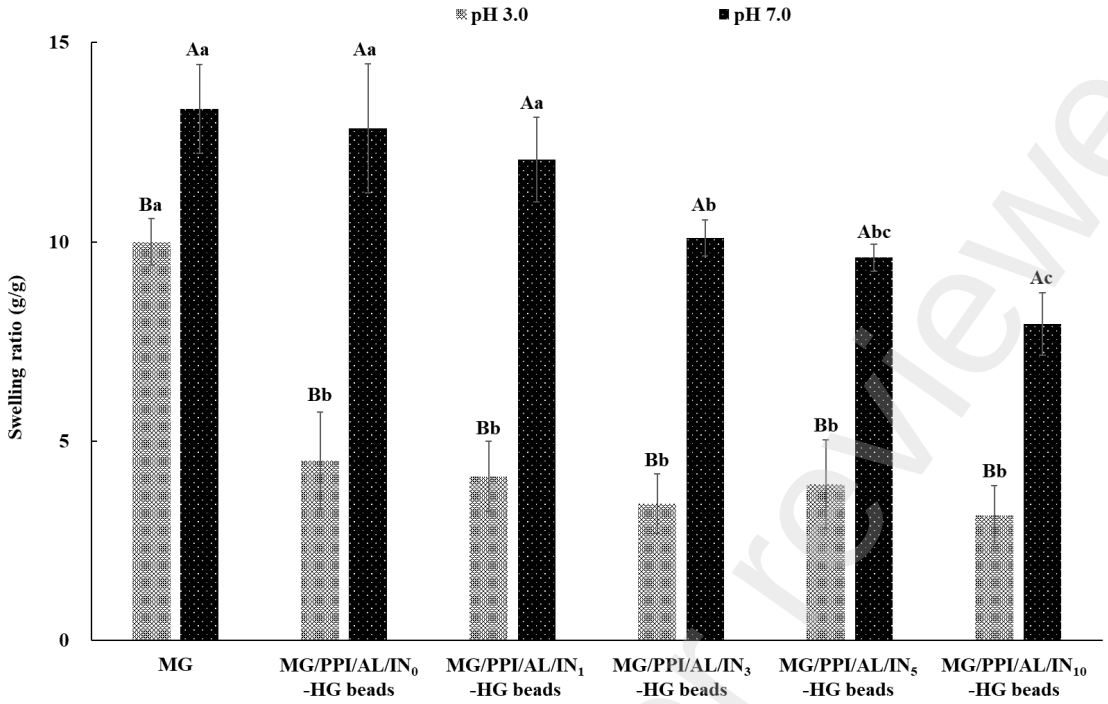

Fig. 5. Swelling ratio of microgels (MG) and core-shell hydrogel beads prepared with different concentrations of inulin (IN). MG/PPI/AL/IN_0-HG beads, MG/PPI/AL/IN_1-HG beads, MG/PPI/AL/IN_3-HG beads, MG/PPI/AL/IN_5-HG beads, and MG/PPI/AL/IN_{10}-HG beads represent core-shell hydrogel beads prepared with different concentrations of IN (0%, 1%, 3%, 5%, and 10%, respectively). Lowercase letters show significant differences among samples at the same pH (p<0.05) and capital letters show significant differences between pH for the same sample (p<0.05).

3.7. *In vitro* release study of encapsulated vitamin B12 in simulated gastrointestinal conditions

It is well known that vitamin B12 is predominantly absorbed in the distal part of the small intestine, although it is unstable in acidic gastric conditions (TemovaRakuša, Roškar, Hickey, & Geremia, 2022). Vitamin B12 should be protected from acid degradation when exposed to gastric conditions and released upon reaching the intestinal conditions (Mazzocato et al., 2019).

The cumulative release of vitamin B12 in MG and core-shell hydrogel beads during *in vitro* digestion is described in Fig. 6. After exposure to simulated oral conditions, the cumulative release of vitamin B12 in MG and core-shell hydrogel beads was negligible. After exposure to simulated gastric conditions for 2 h, most of vitamin B12 was released from MG. However, the cumulative release of vitamin B12 in core-shell hydrogel beads was much lower than that of MG, suggesting that the PPI/AL hydrogel matrix provided an additional barrier to prevent the release of vitamin B12 under simulated gastric conditions. Li et al. (2017) developed whey protein microgels that incorporated AL hydrogels to encapsulate probiotics and reported that core-shell hydrogels provided an additional barrier to protect probiotics under simulated gastric conditions. As a result, it was suggested in this study that the additional hydrogel beads layer, as an extra physical barrier, was able to prevent the release of vitamin B12 from core-shell hydrogel beads and access to digestion fluids (pepsin and gastric acids) under simulated oral and gastric conditions.

The cumulative release of vitamin B12 in MG/PPI/AL_0-HG beads, MG/PPI/AL_1-HG beads, MG/PPI/AL_3-HG beads, MG/PPI/AL_5-HG beads, and MG/PPI/AL_{10}-HG beads under simulated gastric conditions were 50.10%, 45.52%, 40.20%, 35.57%, and 32.92%, respectively. According to the result of the swelling ratio analysis previously mentioned, the swelling of PPI/AL hydrogel beads was restricted at pH 3.0. Furthermore, based on the FE-SEM and FT-IR analysis results, IN can act as filling/coating materials to make the core-shell hydrogel beads denser and have fewer pores by filling and coating the matrix via hydrogen bonds. Liu et al. (2022) reported that adding IN to the AL-chitosan hydrogel beads can delay the release of quercetin under simulated gastric conditions. Córdoba et al. (2013) also reported that adding starch into AL hydrogel beads as filling/coating materials can delay the release of encapsulated nutraceuticals from hydrogel beads under simulated gastric conditions.

Therefore, in the present study, the reduction in the cumulative release of vitamin B12 with increasing concentrations of IN can be related to the formation of a more compact internal structure and surface in core-shell hydrogel beads.

Under the simulated intestinal conditions, most vitamin B12 was released in the core-shell hydrogel beads. The release of vitamin B12 in core-shell hydrogel beads under simulated intestinal conditions may be attributed to the electrostatic repulsion between deprotonated carboxyl groups ($–COO^-$) of PPI and AL. As previously mentioned in the swelling ratio analysis, the swelling ratio of core-shell hydrogel beads at pH 7.0 increased due to electrostatic repulsion between the deprotonated carboxyl groups of PPI and AL. Apoorva, Rameshbabu, Dasgupta, Dhara, & Padmavati (2020) noted that the deprotonated carboxyl groups in AL induced electrostatic repulsion at pH 7.0, consequently leading to the swelling of AL hydrogel beads and the release of phenolic compounds in AL hydrogel beads.

MG/PPI/AL_0-HG beads, MG/PPI/AL_1-HG beads, MG/PPI/AL_3-HG beads, MG/PPI/AL_5-HG beads, and MG/PPI/AL_{10}-HG beads released most of vitamin B12 after exposure to simulated intestinal conditions for 60 min, 60 min, 90 min, 120 min, and 120 min, respectively. These findings indicated that the addition of IN can prevent the burst release and lead to the sustained and prolonged release of vitamin B12 in core-shell hydrogel beads. Wang et al. (2021) observed that the addition of resistant starch into GG hydrogel decreased the release rate of resveratrol under simulated intestinal conditions. They (Wang et al., 2021) reported that these results were attributed to the weakening effects of resistant starch on electrostatic repulsion forces between carboxyl groups. As previously mentioned in the swelling ratio analysis, IN may reduce electrostatic repulsion among anionic groups of PPI and AL, preventing core-shell hydrogel beads from swelling. Additionally, IN was able to make the core-shell hydrogel beads a more densified internal structure and surface with fewer pores (Fig. 1). Therefore, it was indicated that the additional layer filled/coated with IN was able to make sustained and prolonged release of vitamin B12 under simulated intestinal conditions.

Based on the above results, it was demonstrated that providing an additional hydrogel beads layer to MG and filling/coating with IN into PPI/AL hydrogel beads can protect vitamin B12 under simulated gastric conditions and control the cumulative release of vitamin B12 under simulated intestinal

conditions. In particular, MG/PPI/AL/IN_{10}-HG beads exhibited the most stable and sustained release profile, indicating that they can be used as a promising carrier for a controlled-release delivery system for vitamin B12.

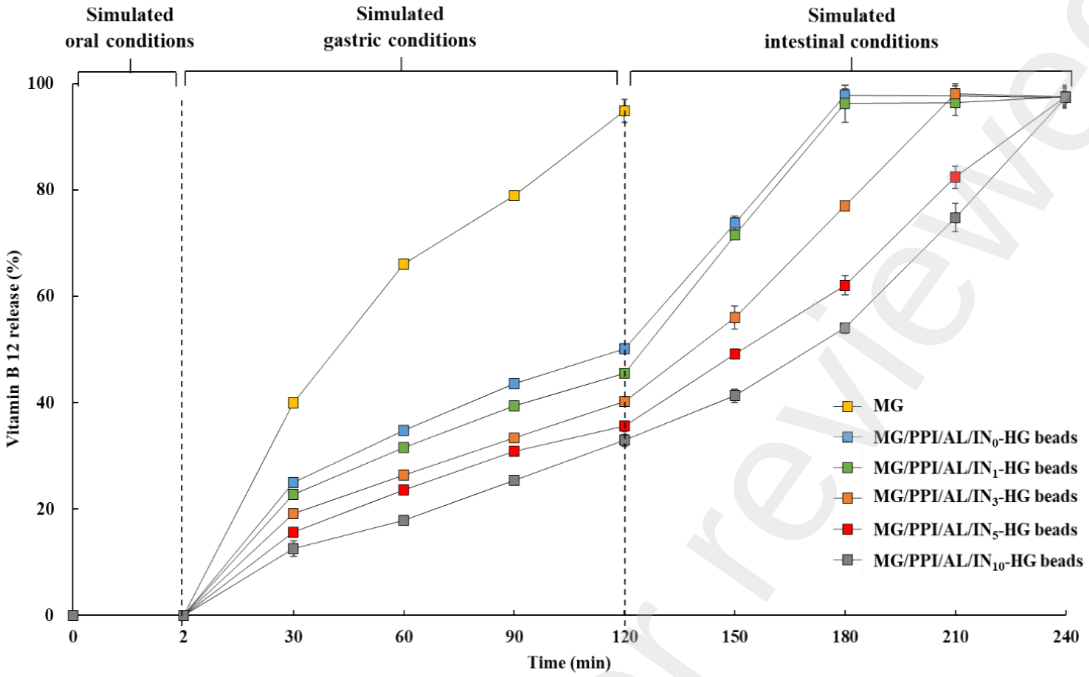

510
511 **Fig. 6.** Cumulative release properties of vitamin B12 in microgels (MG) and core-shell hydrogel beads
512 prepared with different concentrations of inulin (IN) in simulated oral, gastric, and intestinal conditions.
513 MG/PPI/AL/IN_0-HG beads, MG/PPI/AL/IN_1-HG beads, MG/PPI/AL/IN_3-HG beads, MG/PPI/AL/IN_5-
514 HG beads, and MG/PPI/AL/IN_{10}-HG beads represent core-shell hydrogel beads prepared with different
515 concentrations of IN (0%, 1%, 3%, 5%, and 10%, respectively).
516

3.8. Storage stability

The results of the storage stability of vitamin B12 in MG and core-shell hydrogel beads at 4 °C for 7 days and 14 days are shown in Fig. 7. The retention of vitamin B12 in MG was 59.73% and 33.10% after storage for 7 days and 14 days, respectively. However, the retention of vitamin B12 in core-shell hydrogel beads was much higher than that of MG. Chen et al. (2020) reported that the core-shell hydrogels, zein microgels (core), and carrageenan hydrogels (shell) improved the storage stability of coenzyme Q10 and piperine, which indicated that an additional hydrogel shell could protect them from environmental stress. As a result, the present study suggested that core-shell hydrogel beads provided an extra physical barrier (PPI/AL hydrogel beads) to MG and prevented the release of vitamin B12 during storage.

In addition, the retention of vitamin B12 in core-shell hydrogel beads was increased with increasing the concentration of IN. According to the result of the previously mentioned FE-SEM analysis, IN can densify the internal structure and reduce the surface pores of core-shell hydrogel beads. Accordingly, it was assumed that IN inhibited the release of vitamin B12 during storage by filling/coating the core-shell hydrogel beads. This result was in accordance with Tarifa, Piqueras, Genovese, & Brugnoni (2021), who reported that adding IN into pectin microgels enhanced the storage stability of probiotics for 42 days.

Based on the above results, it was suggested that core-shell hydrogel beads filled/coated with IN can enhance the storage stability of encapsulated vitamin B12. Moreover, MG/PPI/AL/IN_{10}-HG beads can be used as an effective system for protecting vitamin B12 against environmental stress.

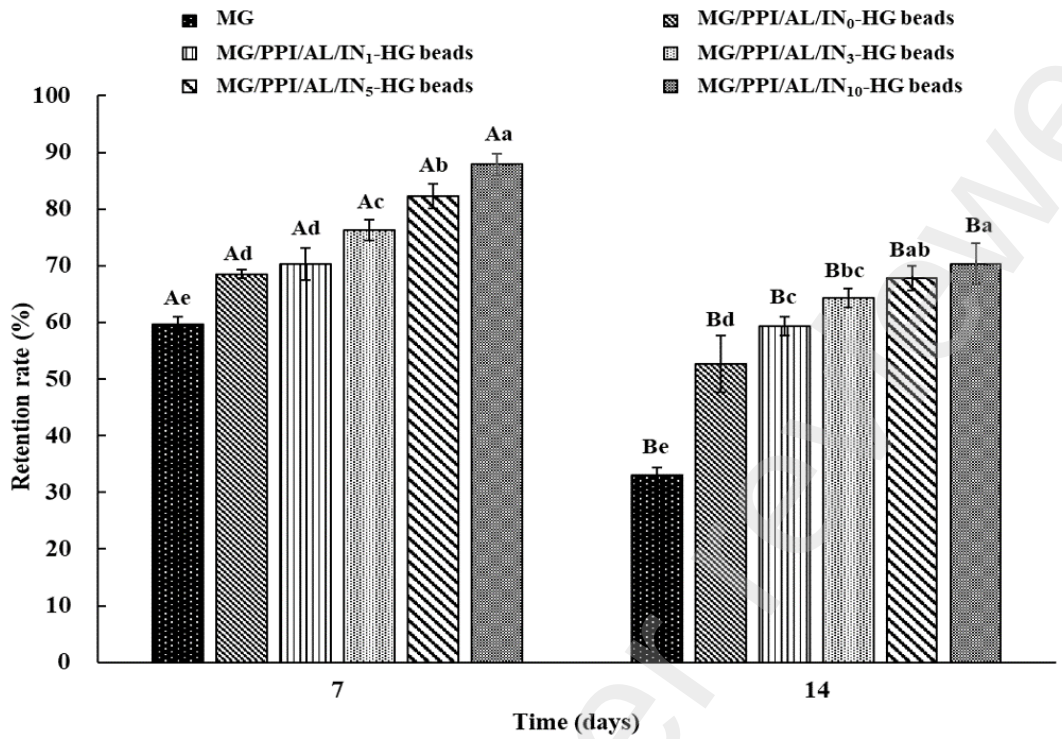

538

539 **Fig**. 7. Storage stability of vitamin B12 in microgels (MG) and core-shell hydrogel beads prepared with
540 different concentrations of inulin (IN). MG/PPI/AL/IN_0-HG beads, MG/PPI/AL/IN_1-HG beads,
541 MG/PPI/AL/IN_3-HG beads, MG/PPI/AL/IN_5-HG beads, and MG/PPI/AL/IN_{10}-HG beads represent
542 core-shell hydrogel beads prepared with different concentrations of IN (0%, 1%, 3%, 5%, and 10%,
543 respectively). Lowercase letters show significant differences among samples at the same time (p<0.05)
544 and capital letters show significant differences among times for the same sample (p<0.05).

545

4. Conclusion

The present study produced core-shell hydrogel beads filled/coated with different concentrations of IN as a controlled-release delivery system for vitamin B12. As proven by the XRD analysis, core-shell hydrogel beads were successfully prepared, and MG was incorporated into them. Based on the results obtained from FE-SEM, FT-IR, and encapsulation efficiency analysis, IN reduced the surface pores and densified the internal structure of core-shell hydrogel beads by filling/coating the matrix via hydrogen bonds, resulting in the enhancement of the encapsulation efficiency of vitamin B12. According to the results of *in vitro* release properties, after sequential exposure to simulated oral and gastric conditions, core-shell hydrogel beads inhibited the release of vitamin B12 by providing a physical barrier to MG. In addition, the release of vitamin B12 was significantly reduced by filling/coating the core-shell hydrogel beads as IN concentration increased. After exposure to simulated intestinal conditions, core-shell hydrogel beads released most of vitamin B12. Besides, the addition of IN was able to sustain and prolong the release of vitamin B12 under simulated intestinal conditions. Based on the *in vitro* release study of vitamin B12 in simulated gastrointestinal conditions, MG/PPI/AL/IN_{10}-HG beads were the most effective matrix for delivering vitamin B12 to intestinal conditions. Furthermore, MG/PPI/AL/IN_{10}-HG beads exhibited the highest storage stability among all samples. In conclusion, this study developed a novel controlled-release delivery system for vitamin B12 in the functional food industry and introduced a method for encapsulating hydrophilic compounds using core-shell hydrogels with filling/coating materials.

Acknowledgments

This research was supported by the National Research Foundation of Korea (NRF) grant funded by the Korea government (MSIT) (No. 2023R1A2C1003093)

References

Afinjuomo, F., Barclay, T. G., Song, Y., Parikh, A., Petrovsky, N., & Garg, S. (2019). Synthesis and characterization of a novel inulin hydrogel crosslinked with pyromellitic dianhydride. Reactive and Functional Polymers, 134, 104-111. https://doi.org/10.1016/j.reactfunctpolym.2018.10.014

Apolinário, A. C., de Carvalho, E. M., de Lima Damasceno, B. P. G., da Silva, P. C. D., Converti, A., Pessoa Jr, A., & da Silva, J. A. (2017). Extraction, isolation and characterization of inulin from Agave sisalana boles. Industrial Crops and Products, 108, 355-362. https://doi.org/10.1016/j.indcrop.2017.06.045

Apoorva, A., Rameshbabu, A. P., Dasgupta, S., Dhara, S., & Padmavati, M. (2020). Novel pH-sensitive alginate hydrogel delivery system reinforced with gum tragacanth for intestinal targeting of nutraceuticals. International journal of biological macromolecules, 147, 675-687. https://doi.org/10.1016/j.ijbiomac.2020.01.027

Balanč, B., Kalušević, A., Drvenica, I., Coelho, M. T., Djordjević, V., Alves, V. D., & Bugarski, B. (2016). Calcium–alginate–inulin microbeads as carriers for aqueous carqueja extract. Journal of Food Science, 81(1), E65-E75. https://doi.org/10.1111/1750-3841.13167

Bayat, M., & Nasri, S. (2019). Injectable microgel–hydrogel composites “plum pudding gels”: New system for prolonged drug delivery. In Nanomaterials for Drug Delivery and Therapy (pp. 343-372). William Andrew Publishing. https://doi.org/10.1016/B978-0-12-816505-8.00001-1

Bishnoi, S., Trvifol, J., Moriana, R., & Mendes, A. C. (2022). Adjustable polysaccharides-proteins films made of aqueous wheat proteins and alginate solutions. Food Chemistry, 391, 133196. https://doi.org/10.1016/j.foodchem.2022.133196

Bonifacio, M. A., Gentile, P., Ferreira, A. M., Cometa, S., & De Giglio, E. (2017). Insight into halloysite nanotubes-loaded gellan gum hydrogels for soft tissue engineering applications. Carbohydrate Polymers, 163, 280-291. https://doi.org/10.1016/j.carbpol.2017.01.064

Brodkorb, A., Egger, L., Alminger, M., Alvito, P., Assunção, R., Ballance, S., ... & Recio, I. (2019). INFOGEST static in vitro simulation of gastrointestinal food digestion. Nature protocols, 14(4), 991-1014. https://doi.org/10.1038/s41596-018-0119-1

Bušić, A., Belščak-Cvitanović, A., Cebin, A. V., Karlović, S., Kovač, V., Špoljarić, I., ... & Komes, D. (2018). Structuring new alginate network aimed for delivery of dandelion (Taraxacum officinale L.) polyphenols using ionic gelation and new filler materials. Food Research International, 111, 244-255. https://doi.org/10.1016/j.foodres.2018.05.034

Byeon, J. H., Kang, Y. R., & Chang, Y. H. (2023). Physicochemical and in vitro digestion properties of gelatin/low-methoxyl pectin synbiotic microgels co-encapsulating Lacticaseibacillus casei and pectic oligosaccharides via double-crosslinking with transglutaminase and calcium ions. Food Hydrocolloids, 142, 108757. https://doi.org/10.1016/j.foodhyd.2023.108757.

Chan, E. S., Wong, S. L., Lee, P. P., Lee, J. S., Ti, T. B., Zhang, Z., &Yim, Z. H. (2011). Effects of starch filler on the physical properties of lyophilized calcium–alginate beads and the viability of encapsulated cells. Carbohydrate Polymers, 83(1), 225-232. https://doi.org/10.1016/j.carbpol.2010.07.044

Chen, S., Zhang, Y., Qing, J., Han, Y., McClements, D. J., & Gao, Y. (2020). Core-shell nanoparticles for co-encapsulation of coenzyme Q10 and piperine: Surface engineering of hydrogel shell around protein core. Food Hydrocolloids, 103, 105651. https://doi.org/10.1016/j.foodhyd.2020.105651

Comunian, T. A., Thomazini, M., Alves, A. J. G., de Matos Junior, F. E., de Carvalho Balieiro, J. C., & Favaro-Trindade, C. S. (2013). Microencapsulation of ascorbic acid by complex coacervation: Protection and controlled release. Food Research International, 52(1), 373-379. https://doi.org/10.1016/j.foodres.2013.03.028

Córdoba, A. L., Deladino, L., & Martino, M. (2013). Effect of starch filler on calcium-alginate hydrogels loaded with yerba mate antioxidants. Carbohydrate Polymers, 95(1), 315-323. https://doi.org/10.1016/j.carbpol.2013.03.019

Cortés-Camargo, S., Román-Guerrero, A., Alvarez-Ramirez, J., Alpizar-Reyes, E., Velázquez-Gutiérrez, S. K., & Pérez-Alonso, C. (2023). Microstructural influence on physical properties and release profiles of sesame oil encapsulated into sodium alginate-tamarind mucilage hydrogel beads. Carbohydrate Polymer Technologies and Applications, 5, 100302. https://doi.org/10.1016/j.carpta.2023.100302

Cortez-Trejo, M. C., Loarca-Piña, G., Figueroa-Cárdenas, J. D., Manríquez, J., & Mendoza, S. (2022). Gel properties of acid-induced gels obtained at room temperature and based on common bean proteins and xanthan gum. Food Hydrocolloids, 132, 107873. https://doi.org/10.1016/j.foodhyd.2022.107873

De Berardinis, L., Plazzotta, S., & Manzocco, L. (2023). Optimising Soy and Pea Protein Gelation to Obtain Hydrogels Intended as Precursors of Food-Grade Dried Porous Materials. Gels, 9(1), 62. https://doi.org/10.3390/gels9010062

de Souza, F. S., de Mello Ferreira, I. L., da Silva Costa, M. A., de Lima, A. L. F., da Costa, M. P. M., & da Silva, G. M. (2016). Evaluation of different methods to prepare superabsorbent hydrogels based on deacetylated gellan. Carbohydrate Polymers, 148, 309-317. https://doi.org/10.1016/j.carbpol.2016.04.019

Dutta, S., & Bhattacharjee, P. (2017). Nanoliposomal encapsulates of piperine-rich black pepper extract obtained by enzyme-assisted supercritical carbon dioxide extraction. Journal of Food Engineering, 201, 49-56. https://doi.org/10.1016/j.jfoodeng.2017.01.006

Ellis, A., &Jacquier, J. C. (2009). Manufacture of food grade κ-carrageenan microspheres. Journal of Food Engineering, 94(3-4), 316-320. https://doi.org/10.1016/j.jfoodeng.2009.03.030

Estevinho, B. N., Carlan, I., Blaga, A., & Rocha, F. (2016). Soluble vitamins (vitamin B12 and vitamin C) microencapsulated with different biopolymers by a spray drying process. Powder Technology, 289, 71-78. https://doi.org/10.1016/j.powtec.2015.11.019

Fan, Z., Cheng, P., Zhang, P., Zhang, G., & Han, J. (2022). Rheological insight of polysaccharide/protein based hydrogels in recent food and biomedical fields: A review. International Journal of Biological Macromolecules. https://doi.org/10.1016/j.ijbiomac.2022.10.082

Fang, J., Jiang, F., Xu, X., Xiao, Q., Yang, Q., Chen, F., & Xiao, A. (2023). Gelation melioration with synergistic interaction between κ-carrageenan and senna tora gum mixed gel. Food Hydrocolloids, 109574. https://doi.org/10.1016/j.foodhyd.2023.109574

Farjami, T., & Madadlou, A. (2017). Fabrication methods of biopolymeric microgels and microgel-based hydrogels. Food Hydrocolloids, 62, 262-272. https://doi.org/10.1016/j.foodhyd.2016.08.017

650 Girard, C. L., Santschi, D. E., Stabler, S. P., & Allen, R. H. (2009). Apparent ruminal synthesis and
651 intestinal disappearance of vitamin B12 and its analogs in dairy cows. Journal of Dairy Science, 92(9),
652 4524-4529. https://doi.org/10.3168/jds.2009-2049
653 Lee, Y. E., Kang, Y. R., & Chang, Y. H. (2023). Effect of pectic oligosaccharide on probiotic survival
654 and physicochemical properties of hydrogel beads for synbiotic encapsulation of Lactobacillus
655 bulgaricus. Food Bioscience, 51, 102260. https://doi.org/10.1016/j.fbio.2022.102260
656 Gómez-Mascaraque, L. G., Soler, C., & Lopez-Rubio, A. (2016). Stability and bioaccessibility of
657 EGCG within edible micro-hydrogels. Chitosan vs. gelatin, a comparative study. Food Hydrocolloids,
658 61, 128-138. https://doi.org/10.1016/j.foodhyd.2016.05.009
659 Guo, Q., Su, J., Xie, W., Tu, X., Yuan, F., Mao, L., & Gao, Y. (2020). Curcumin-loaded pea protein
660 isolate-high methoxyl pectin complexes induced by calcium ions: Characterization, stability and in vitro
661 digestibility. Food Hydrocolloids, 98, 105284. https://doi.org/10.1016/j.foodhyd.2019.105284
662 Ionita, M., Pandele, M. A., & Iovu, H. (2013). Sodium alginate/graphene oxide composite films with
663 enhanced thermal and mechanical properties. Carbohydrate Polymers, 94(1), 339-344.
664 https://doi.org/10.1016/j.carbpol.2013.01.065
665 Ji, X., Yin, M., Hao, L., Shi, M., Liu, H., & Liu, Y. (2021). Effect of inulin on pasting, thermal,
666 rheological properties and in vitro digestibility of pea starch gel. International Journal of Biological
667 Macromolecules, 193, 1669-1675. https://doi.org/10.1016/j.ijbiomac.2021.11.004
668 Jin, L., Lu, P., You, H., Chen, Q., & Dong, J. (2009). Vitamin B12 diffusion and binding in
669 crosslinked poly (acrylic acid) s and poly (acrylic acid-co-N-vinyl pyrrolidinone) s. International
670 Journal of Pharmaceutics, 371(1-2), 82-88. https://doi.org/10.1016/j.ijpharm.2008.12.022
671 Karthika, J. S., Vishalakshi, B., & Naik, J. (2016). Gellan gum–graft–polyaniline—An electrical
672 conducting biopolymer. International Journal of Biological Macromolecules, 82, 61-67.
673 https://doi.org/10.1016/j.ijbiomac.2015.10.061
674 Kaur, K., Jindal, R., & Jindal, D. (2020). Controlled release of vitamin B1 and evaluation of
675 biodegradation studies of chitosan and gelatin based hydrogels. International Journal of Biological
676 Macromolecules, 146, 987-999. https://doi.org/10.1016/j.ijbiomac.2019.09.223

677 Khodaverdi, E., Tekie, F. S. M., Hadizadeh, F., Esmaeel, H., Mohajeri, S. A., Tabassi, S. A. S., &
678 Zohuri, G. (2014). Hydrogels composed of cyclodextrin inclusion complexes with PLGA-PEG-PLGA
679 triblock copolymers as drug delivery systems. Aaps Pharmscitech, 15, 177-188.
680 https://doi.org/10.1208/s12249-013-0051-1
681 Kozyraki, R., & Cases, O. (2013). Vitamin B12 absorption: mammalian physiology and acquired and
682 inherited disorders. Biochimie, 95(5), 1002-1007. https://doi.org/10.1016/j.biochi.2012.11.004
683 Kurozawa, L. E., & Hubinger, M. D. (2017). Hydrophilic food compounds encapsulation by ionic
684 gelation. Current Opinion in Food Science, 15, 50-55. https://doi.org/10.1016/j.cofs.2017.06.004
685 Li, Y., Feng, C., Li, J., Mu, Y., Liu, Y., Kong, M., ... & Chen, X. (2017). Construction of multilayer
686 alginate hydrogel beads for oral delivery of probiotics cells. International journal of biological
687 macromolecules, 105, 924-930. https://doi.org/10.1016/j.ijbiomac.2017.07.124
688 Li, Q., Duan, M., Hou, D., Chen, X., Shi, J., & Zhou, W. (2021). Fabrication and characterization of
689 Ca (II)-alginate-based beads combined with different polysaccharides as vehicles for delivery, release
690 and storage of tea polyphenols. Food Hydrocolloids, 112, 106274.
691 https://doi.org/10.1016/j.foodhyd.2020.106274
692 Li, Q., Li, X., & Zhao, C. (2020). Strategies to obtain encapsulation and controlled release of small
693 hydrophilic molecules. Frontiers in Bioengineering and Biotechnology, 8, 437.
694 https://doi.org/10.3389/fbioe.2020.00437
695 Liu, S., Fang, Z., & Ng, K. (2022). Incorporating inulin and chitosan in alginate-based microspheres
696 for targeted delivery and release of quercetin to colon. Food Research International, 160, 111749.
697 https://doi.org/10.1016/j.foodres.2022.111749
698 Lopes, S. C., Gadelha, D. D., Carvalho, M. D. D., Fernandes, V. O., & Montenegro Junior, R. M.
699 (2019). Vitamin B12 deficiency: metabolic effects, clinical evaluation, and treatment.
700 http://www.repositorio.ufc.br/handle/riufc/42984
701 López-Molina, D., Chazarra, S., How, C. W., Pruidze, N., Navarro-Perán, E., García-Cánovas, F., &
702 Rodríguez-López, J. N. (2015). Cinnamate of inulin as a vehicle for delivery of colonic drugs.
703 International Journal of Pharmaceutics, 479(1), 96-102. https://doi.org/10.1016/j.ijpharm.2014.12.064

Lu, Z. X., He, J. F., Zhang, Y. C., & Bing, D. J. (2020). Composition, physicochemical properties of pea protein and its application in functional foods. Critical Reviews in Food Science and Nutrition, 60(15), 2593-2605. https://doi.org/10.1080/10408398.2019.1651248

Mahmood, H., Khan, I. U., Asif, M., Khan, R. U., Asghar, S., Khalid, I., & Asim, M. (2021). In vitro and in vivo evaluation of gellan gum hydrogel films: Assessing the co impact of therapeutic oils and ofloxacin on wound healing. International Journal of Biological Macromolecules, 166, 483-495. https://doi.org/10.1016/j.ijbiomac.2020.10.206

Mazzocato, M. C., Thomazini, M., & Favaro-Trindade, C. S. (2019). Improving stability of vitamin B12 (Cyanocobalamin) using microencapsulation by spray chilling technique. Food Research International, 126, 108663. https://doi.org/10.1016/j.foodres.2019.108663

McClements, D. J. (2015). Encapsulation, protection, and release of hydrophilic active components: Potential and limitations of colloidal delivery systems. Advances in Colloid and Interface Science, 219, 27-53. https://doi.org/10.1016/j.cis.2015.02.002

Message, J. L., Blanchard, C., Mint-Dah, F. V., Lafarge, C., Assifaoui, A., & Saurel, R. (2013). The effects of sodium alginate and calcium levels on pea proteins cold-set gelation. Food Hydrocolloids, 31(2), 446-457. https://doi.org/10.1016/j.foodhyd.2012.11.004

Mirmazloum, I., Ladányi, M., Omran, M., Papp, V., Ronkainen, V. P., Pónya, Z., ... & Kiss, A. (2021). Co-encapsulation of probiotic Lactobacillus acidophilus and Reishi medicinal mushroom (Ganoderma lingzhi) extract in moist calcium alginate beads. International journal of biological macromolecules, 192, 461-470. https://doi.org/10.1016/j.ijbiomac.2021.09.177

Moon, E. C., & Chang, Y. H. (2022). Physicochemical, Structural, and In Vitro Gastrointestinal Tract Release Properties of Sodium Alginate-Based Cryogel Beads Filled with Hydroxypropyl Distarch Phosphate as a Curcumin Delivery System. Molecules, 28(1), 31. https://doi.org/10.3390/molecules28010031

Morkbak, A. L., Poulsen, S. S., & Nexo, E. (2007). Haptocorrin in humans. https://doi.org/10.1515/CCLM.2007.343

730 Mozafarpour, R., & Koocheki, A. (2023). Effect of ultrasonic pretreatment on the rheology and
731 structure of grass pea (Lathyrus sativus L.) protein emulsion gels induced by transglutaminase.
732 Ultrasonics Sonochemistry, 92, 106278. https://doi.org/10.1016/j.ultsonch.2022.106278
733 Mundlia, J., Ahuja, M., & Kumar, P. (2021). Enhanced biological activity of polyphenols on
734 conjugation with gellan gum. International Journal of Polymeric Materials and Polymeric Biomaterials,
735 70(10), 712-729. https://doi.org/10.1080/00914037.2020.1760273
736 Nascimento, L. G. L., Casanova, F., Silva, N. F. N., de Carvalho Teixeira, Á. V. N., Júnior, P. P. D.
737 S. P., Vidigal, M. C. T. R., ... & de Carvalho, A. F. (2020). Use of a crosslinked casein micelle hydrogel
738 as a carrier for jaboticaba (Myrciaria cauliflora) extract. Food Hydrocolloids, 106, 105872.
739 https://doi.org/10.1016/j.foodhyd.2020.105872
740 O'Leary, F., & Samman, S. (2010). Vitamin B12 in health and disease. Nutrients, 2(3), 299-316.
741 https://doi.org/10.3390/nu2030299
742 Ozel, B., Zhang, Z., He, L., & McClements, D. J. (2020). Digestion of animal-and plant-based
743 proteins encapsulated in κ-carrageenan/protein beads under simulated gastrointestinal conditions. Food
744 Research International, 137, 109662. https://doi.org/10.1016/j.foodres.2020.109662
745 Paliwal, R., & Palakurthi, S. (2014). Zein in controlled drug delivery and tissue engineering. Journal
746 of Controlled Release, 189, 108-122. https://doi.org/10.1016/j.jconrel.2014.06.036
747 Panchev, I., Delchev, N., Kovacheva, D., & Slavov, A. (2011). Physicochemical characteristics of
748 inulins obtained from Jerusalem artichoke (Helianthus tuberosus L.). European Food Research and
749 Technology, 233, 889-896. https://doi.org/10.1007/s00217-011-1584-8
750 Rathna, G. V. N., Birajdar, M. S., Bhagwani, M., & Paul, V. L. (2013). Studies on fabrication,
751 characterization, and metal extraction using metal chelating nonwoven nanofiber mats of poly (vinyl
752 alcohol) and sodium alginate blends. Polymer Engineering & Science, 53(2), 321-333.
753 https://doi.org/10.1002/pen.23267
754 Rizzo, G., & Laganà, A. S. (2020). A review of vitamin B12. Molecular nutrition, 105-129.
755 https://doi.org/10.1016/B978-0-12-811907-5.00005-1

Ronkart, S. N., Paquot, M., Fougnies, C., Deroanne, C., & Blecker, C. S. (2009). Effect of water uptake on amorphous inulin properties. Food hydrocolloids, 23(3), 922-927. https://doi.org/10.1016/j.foodhyd.2008.06.003

Saavedra-Leos, M. Z., Leyva-Porras, C., Martínez-Guerra, E., Pérez-García, S. A., Aguilar-Martínez, J. A., & Álvarez-Salas, C. (2014). Physical properties of inulin and inulin–orange juice: Physical characterization and technological application. Carbohydrate Polymers, 105, 10-19. https://doi.org/10.1016/j.carbpol.2013.12.079

Sarti, F., Müller, C., Iqbal, J., Perera, G., Laffleur, F., & Bernkop-Schnürch, A. (2013). Development and in vivo evaluation of an oral vitamin B12 delivery system. European Journal of Pharmaceutics and Biopharmaceutics, 84(1), 132-137. https://doi.org/10.1016/j.ejpb.2012.11.024

Shevkani, K., Singh, N., Kaur, A., & Rana, J. C. (2015). Structural and functional characterization of kidney bean and field pea protein isolates: A comparative study. Food Hydrocolloids, 43, 679-689. https://doi.org/10.1016/j.foodhyd.2014.07.024

Shipton, M. J., & Thachil, J. (2015). Vitamin B12 deficiency–A 21st century perspective. Clinical Medicine, 15(2), 145. https://doi.org/10.7861/clinmedicine.15-2-145

Smith, A. D., Warren, M. J., & Refsum, H. (2018). Vitamin B12. Advances in Food and Nutrition Research, 83, 215-279. https://doi.org/10.1016/bs.afnr.2017.11.005

Stabler, S. P. (2013). Vitamin B12 deficiency. New England Journal of Medicine, 368(2), 149-160. https://doi.org/10.1056/NEJMcp1113996

Stojanovic, R., Belscak-Cvitanovic, A., Manojlovic, V., Komes, D., Nedovic, V., & Bugarski, B. (2012). Encapsulation of thyme (Thymus serpyllum L.) aqueous extract in calcium alginate beads. Journal of the Science of Food and Agriculture, 92(3), 685-696. https://doi.org/10.1002/JSFA.4632

Tan, C., Arshadi, M., Lee, M. C., Godec, M., Azizi, M., Yan, B., ... & Abbaspourrad, A. (2019). A robust aqueous core–shell–shell coconut-like nanostructure for stimuli-responsive delivery of hydrophilic cargo. ACS nano, 13(8), 9016-9027. https://doi.org/10.1021/acsnano.9b03049

Tarifa, M. C., Piqueras, C. M., Genovese, D. B., & Brugnoni, L. I. (2021). Microencapsulation of Lactobacillus casei and Lactobacillus rhamnosus in pectin and pectin-inulin microgel particles: Effect

783 on bacterial survival under storage conditions. International Journal of Biological Macromolecules, 179,
784 457-465. https://doi.org/10.1016/j.ijbiomac.2021.03.038
785 TemovaRakuša, Ž., Roškar, R., Hickey, N., & Geremia, S. (2022). Vitamin B12 in Foods, Food
786 Supplements, and Medicines—A Review of Its Role and Properties with a Focus on Its Stability.
787 Molecules, 28(1), 240. https://doi.org/10.3390/molecules28010240
788 Wang, H., Shou, Y., Zhu, X., Xu, Y., Shi, L., Xiang, S., ... & Han, J. (2019). Stability of vitamin B12
789 with the protection of whey proteins and their effects on the gut microbiome. Food Chemistry, 276,
790 298-306. https://doi.org/10.1016/j.foodchem.2018.10.033
791 Wang, P., Luo, Z. G., & Xiao, Z. G. (2021). Preparation, physicochemical characterization and in
792 vitro release behavior of resveratrol-loaded oxidized gellan gum/resistant starch hydrogel beads.
793 Carbohydrate Polymers, 260, 117794. https://doi.org/10.1016/j.carbpol.2021.117794
794 Wang, Y., Jiao, A., Qiu, C., Liu, Q., Yang, Y., Bian, S., & Jin, Z. (2022). A combined enzymatic and
795 ionic crosslinking strategy for pea protein/sodium alginate double-network hydrogel with excellent
796 mechanical properties and freeze-thaw stability. Food Hydrocolloids, 131, 107737.
797 https://doi.org/10.1016/j.foodhyd.2022.107737
798 Wu, S., Wang, L., Zhao, Y., Chen, B., Qiu, D., Sun, P., & Feng, S. (2023). Fabrication of high strength
799 cold-set sodium alginate/whey protein nanofiber double network hydrogels and their interaction with
800 curcumin. Food Research International, 165, 112490. https://doi.org/10.1016/j.foodres.2023.112490
801 Xu, M., & Dumont, M. J. (2015). Evaluation of the stability of pea and canola protein-based
802 hydrogels in simulated gastrointestinal fluids. Journal of Food Engineering, 165, 52-59.
803 https://doi.org/10.1016/j.jfoodeng.2015.04.033
804 Yang, J., Liang, G., Xiang, T., & Situ, W. (2021). Effect of crosslinking processing on the chemical
805 structure and biocompatibility of a chitosan-based hydrogel. Food Chemistry, 354, 129476.
806 https://doi.org/10.1016/j.foodchem.2021.129476
807 Yao, M., Wu, J., Li, B., Xiao, H., McClements, D. J., & Li, L. (2017). Microencapsulation of
808 Lactobacillus salivarious Li01 for enhanced storage viability and targeted delivery to gut microbiota.
809 Food Hydrocolloids, 72, 228-236. https://doi.org/10.1016/j.foodhyd.2017.05.033

Zhou, F. F., Pan, M. K., Liu, Y., Guo, N., Zhang, Q., & Wang, J. H. (2020). Effects of Na+ on the cold gelation between a low-methoxyl pectin extracted from Premna microphylla turcz and soy protein isolate. Food Hydrocolloids, 104, 105762. https://doi.org/10.1016/j.foodhyd.2020.105762